

Block cross-interactive residual smoothing for Lanczos-type solvers for linear systems with multiple right-hand sides*

Kensuke Aihara[†] Akira Imakura[‡] Keiichi Morikuni[‡]

Abstract

Lanczos-type solvers for large sparse linear systems often exhibit large oscillations in the residual norms. In finite precision arithmetic, large oscillations increase the residual gap (the difference between the recursively updated residual and the explicitly computed residual) and a loss of attainable accuracy of the approximations. This issue is addressed using cross-interactive residual smoothing (CIRS). This approach improves convergence behavior and reduces the residual gap. Similar to how the standard Lanczos-type solvers have been extended to global and block versions for solving systems with multiple right-hand sides, CIRS can also be extended to these versions. While we have developed a global CIRS scheme (GI-CIRS) in our previous study [K. Aihara, A. Imakura, and K. Morikuni, SIAM J. Matrix Anal. Appl., 43 (2022), pp.1308–1330], in this study, we propose a block version (BI-CIRS). Subsequently, we demonstrate the effectiveness of BI-CIRS from various perspectives, such as theoretical insights into the convergence behaviors of the residual and approximation norms, numerical experiments on model problems, and a detailed rounding error analysis for the residual gap. For BI-CIRS, orthonormalizing the columns of direction matrices is crucial in effectively reducing the residual gap. This analysis also complements our previous study and evaluates the residual gap of the block Lanczos-type solvers.

Keywords. multiple right-hand sides, block Lanczos-type solver, residual smoothing, residual gap, inexact orthonormalization

AMS subject classifications. 65F10, 65F25

1 Introduction

In this study, we consider solving large sparse linear systems with multiple right-hand sides

$$AX = B, \quad A \in \mathbb{R}^{n \times n}, \quad B = [\mathbf{b}_1, \mathbf{b}_2, \dots, \mathbf{b}_s] \in \mathbb{R}^{n \times s}, \quad (1)$$

where A is nonsingular and not necessarily symmetric, and the number of right-hand sides s is moderate, that is, $s \ll n$. This study also focuses on block Lanczos-type solvers for the problem (1) and proposes a refined residual smoothing technique for improving their convergence behavior and attainable accuracy of approximations. For a comprehensive discussion, we first outline the background, motivation, and related results of this study.

***Funding:** This study was supported by grant numbers JP20K14356, JP21K11925, 23K21673, 23H00462, JP24K14985 and JP24K00535 from Grants-in-Aid for Scientific Research Program (KAKENHI) of the Japan Society for the Promotion of Science (JSPS).

[†]Department of Computer Science, Faculty of Information Technology, Tokyo City University, 1-28-1 Tamazutsumi, Setagaya-ku, Tokyo 158-8557, Japan (aiharak@tcu.ac.jp).

[‡]Institute of Systems and Information Engineering, University of Tsukuba, 1-1-1 Tennodai, Tsukuba, Ibaraki 305-8573, Japan (imakura@cs.tsukuba.ac.jp, morikuni@cs.tsukuba.ac.jp).

1.1 Application problems

The problem (1) is extensively studied in various scientific computing fields; for instance, numerical simulations of electromagnetic scattering and wave propagation [26, 41, 42, 40], quantum scattering [50], structural mechanics [10, 31], chemistry [5], multiple radiation and scattering problems in structural acoustics [25], and lattice quantum chromodynamics [36, 44]. The problem (1) also arises as a subproblem in numerical methods such as the block Lanczos procedure for eigenvalue problems [6, 14], a block variant of the Jacobi–Davidson method [39], block eliminations by bordering a square matrix with a few rows and columns [12], and other projection-type eigensolvers [18, 19, 32]. These challenges in applications have motivated the community to deeply explore fast and accurate numerical algorithms for solving such problems (1).

1.2 Krylov subspace methods for multiple right-hand sides

This study focuses on using Krylov subspace methods to solve (1). For a single linear system $A\mathbf{x} = \mathbf{b}$ ($\mathbf{b} \in \mathbb{R}^n$), the standard Krylov subspace is defined as follows:

$$\mathcal{K}_k(A, \mathbf{r}_0) := \text{span}(\mathbf{r}_0, A\mathbf{r}_0, \dots, A^{k-1}\mathbf{r}_0), \quad (2)$$

where $\mathbf{r}_0 := \mathbf{b} - A\mathbf{x}_0$ is the initial residual for a given initial guess $\mathbf{x}_0 \in \mathbb{R}^n$. The Krylov subspace has been extended in two ways to simultaneously solve the s linear systems in (1); global and block Krylov subspaces. The global- and block-type solvers have advantages over the standard ones. In the following, let $X_0 \in \mathbb{R}^{n \times s}$ be an initial guess and $R_0 := B - AX_0$ be the corresponding initial residual for (1).

The global-type solvers generate approximations by constructing the following search subspace (often referred to as a matrix Krylov subspace [21]):

$$\mathcal{K}_k^G(A, R_0) := \left\{ \sum_{i=0}^{k-1} c_i A^i R_0 \mid c_i \in \mathbb{R} \right\}, \quad (3)$$

which is a simple extension of (2) for multiple right-hand sides. They can also handle more general linear matrix equations easily and thus have favorable usability. Specific global methods (e.g., see [22, 52]) for (1) correspond to their standard counterparts for $(I_{ns} \otimes A)\hat{\mathbf{x}} = \hat{\mathbf{b}}$, where I_{ns} is the identity matrix of order ns , \otimes denotes the Kronecker product, and $\hat{\mathbf{b}} := [\mathbf{b}_1^\top, \mathbf{b}_2^\top, \dots, \mathbf{b}_s^\top]^\top$. Therefore, the global-type solvers have essentially the same numerical properties as the corresponding standard ones for a single linear system.

The block-type solvers utilize a so-called block Krylov subspace

$$\mathcal{K}_k^\square(A, R_0) := \left\{ \sum_{i=0}^{k-1} A^i R_0 c_i^\square \mid c_i^\square \in \mathbb{R}^{s \times s} \right\}, \quad (4)$$

and a column of the k th approximation X_k is determined with expanding s -dimensional subspace at each iteration. Therefore, this type of method determines approximations more efficiently than the standard and global ones. Note that (4) simplifies to (3) when $c_i^\square := c_i I_s$ for $c_i \in \mathbb{R}$.

As in the standard Krylov subspace methods, most of the global- and block-type solvers are broadly classified into the methods based on the (global or block) Lanczos or Arnoldi process. In the next subsection, we briefly review the specific block Lanczos-type solvers for (1) with $s > 1$.

1.3 Block Lanczos-type solvers

The most basic block-type solver is the block conjugate gradient (Bl-CG) method for symmetric positive definite linear systems (e.g., see [3, 4, 13, 29, 30, 34]). Many block-type solvers for nonsymmetric (or non-Hermitian) linear systems have been developed to extend the capabilities of Bl-CG. These include block versions of BiCG and its associated product-type methods.

The underlying block BiCG (Bl-BiCG) method was presented by O’Leary [30], and its quasi-minimal residual (QMR) variants were developed by Freund and Malhotra [12] and Simoncini [38]. The block BiCG stabilized (Bl-BiCGSTAB) method, which is a representative block product-type BiCG, was proposed by El Guennouni et al. [10]. The block Lanczos/Orthodir and BIODIR methods [11] were also developed by the same authors. Afterward, several modifications of the block-type solvers were studied; for instance, Tadano et al. [45] reformulated Bl-BiCGSTAB as the block BiCG gap-reducing (Bl-BiCGGR) method, and Rashedi et al. [33] modified the block (and global) versions of BiCG, QMR, and BiCGSTAB to improve their numerical stability. Other block product-type BiCG, such as the block BiCGstab(ℓ) [35] and block generalized product-type BiCG (Bl-GPBiCG) [24, 46] methods, were also considered. Moreover, Du et al. [8] developed a block version of the induced dimension reduction (IDR)(s) method, which extends Bl-BiCGSTAB, and Naito et al. [27] proposed its modified variant.

We also remark on the numerical stability of block-type solvers. Unlike the standard- and global-type solvers, the block-type solvers require inversions of $s \times s$ matrices. These matrices can be ill-conditioned as the iteration proceeds, leading to a deterioration in the convergence. To address this issue, we orthonormalize the columns of $n \times s$ iteration matrices. The effectiveness of the orthonormalization strategy has been demonstrated in numerous studies (e.g., see [9, 24, 28, 30, 33, 43]), and such a stabilized implementation is currently the standard approach.

1.4 On the residual gap

An important issue with block-type solvers is the amplification of the residual gap, which can lead to a loss of attainable accuracy of the approximations. This issue is examined in detail below.

For updating the approximation X_k and the corresponding residual R_k , the block-type solvers typically use the recursion formulas

$$X_{k+1} = X_k + P_k \alpha_k^\square, \quad R_{k+1} = R_k - (AP_k) \alpha_k^\square, \quad k = 0, 1, \dots, \quad (5)$$

respectively, where $P_k \in \mathbb{R}^{n \times s}$ is a direction matrix and $\alpha_k^\square \in \mathbb{R}^{s \times s}$ is determined under a certain condition such as orthogonality or minimization. Given the initial residual $R_0 (= B - AX_0)$, the equality $R_k = B - AX_k$ holds for $k = 1, 2, \dots$, in exact arithmetic, but does not necessarily hold in finite precision arithmetic due to rounding errors. Let us introduce the residual gap as follows:

$$G_{R_k} := (B - AX_k) - R_k, \quad (6)$$

where $B - AX_k$ and R_k are the explicitly computed residual (also called true residual) and recurrently updated residual, respectively. Then, the true residual norm can be bounded as follows:

$$\|G_{R_k}\| - \|R_k\| \leq \|B - AX_k\| \leq \|G_{R_k}\| + \|R_k\|. \quad (7)$$

Throughout, $\|\cdot\|$ denotes the Frobenius norm, that is, $\|X\| := \sqrt{\langle X, X \rangle_F}$ with an inner product $\langle X, Y \rangle_F := \text{tr}(X^\top Y)$ for $X, Y \in \mathbb{R}^{n \times s}$. The bounds (7) imply that the attainable accuracy of X_k measured by the true residual norm depends on $\|G_{R_k}\|$ when $\|R_k\|$ becomes sufficiently small. In this study, we propose a refined residual smoothing scheme to suppress an increase in the residual gap and to improve attainable accuracy.

The residual gap for (5) was evaluated in our study [1] assuming that the columns of the direction matrix P_k are exactly orthonormalized. The aforementioned orthonormalization strategy for block-type solvers is related to the residual gap (and our residual smoothing scheme described later). In the following, the column-orthonormal matrix is expressed as Q_k rather than P_k , $\mathbb{F} \subset \mathbb{R}$ is a set of floating point numbers, $\text{fl}(\cdot)$ denotes the result of floating point operations, \mathbf{u} denotes the unit roundoff, and m is the maximum number of nonzero entries per row of A .

Theorem 1.1 ([1, Theorem 2.2]). *In finite precision arithmetic, let $X_k \in \mathbb{F}^{n \times s}$ and $R_k \in \mathbb{F}^{n \times s}$ be the k th approximation and residual, respectively, generated by*

$$X_{k+1} = X_k + Q_k \alpha_k^\square, \quad R_{k+1} = R_k - (AQ_k) \alpha_k^\square, \quad k = 0, 1, \dots, \quad (8)$$

where $X_0 := O$. If the columns of $Q_j \in \mathbb{R}^{n \times s}$ are (exactly) orthonormal for $j < k$, the norm of the residual gap $G_{R_k} = (B - AX_k) - R_k$ is bounded as

$$\|G_{R_k}\| \lesssim k(3 + 4s\sqrt{s} + 2m\sqrt{s})\mathbf{u}\|A\| \max_{0 < j \leq k} \|X_j\| + 3(k+1)\mathbf{u} \max_{0 \leq j \leq k} \|R_j\|.$$

Here, the inequality \lesssim is due to the omission of $\mathcal{O}(\mathbf{u}^2)$ and regarding $\mathbf{u}\|\text{fl}(\cdot)\|$ as $\mathbf{u}\|\cdot\|$.

This theorem implies that large approximation and residual norms contribute to an increase in the residual gap, as is often observed in practice. However, the exact orthonormality assumption for Q_j is scarcely satisfied in finite precision arithmetic. As noted in [1], the bounds on the residual gap remain unclear when performing an inexact orthonormalization to direction matrices. Although it was also remarked in several papers (e.g., see [24, 28, 43]) that the orthonormalization for iteration matrices is effective for reducing the residual gap, only qualitative observations were made and this improvement has not been examined quantitatively via rounding error analysis. Therefore, this study also aims to provide a quantitative evaluation of the residual gap when inexactness is allowed in the orthonormalization; the evaluation will be described in Theorem 4.1.

1.5 Advances in residual smoothing

For the Lanczos-type solvers for a single linear system, residual smoothing introduced by Schönauer [37] is a well-known technique to obtain a non-increasing sequence of residual norms and has been investigated deeply by Weiss [48] and Walker [47]. This technique can also be used to connect different solvers [49]. For instance, Zhou and Walker [53] clarified the connection between BiCG and QMR via residual smoothing and developed the so-called QMR smoothing scheme. In [53], an alternative smoothing implementation was also suggested to enhance numerical stability. Further, the standard residual smoothing was extended for multiple right-hand sides.

Here, we introduce a block version of the simple residual smoothing (Bl-SRS) presented by Jbilou [20] (we refer to Zhang and Dai [51] for the global version). Let $\{X_k\}$ and $\{R_k\}$ denote the primary sequences of approximations and residuals, respectively. With $Y_0 := X_0$ and $S_0 := R_0$, new sequences of approximations Y_k and the corresponding smoothed residuals $S_k (= B - AY_k)$ are generated by the recursion formulas

$$Y_k = Y_{k-1} + (X_k - Y_{k-1})\eta_k^\square, \quad S_k = S_{k-1} + (R_k - S_{k-1})\eta_k^\square, \quad k = 0, 1, \dots, \quad (9)$$

where $\eta_k^\square \in \mathbb{R}^{s \times s}$ is a parameter matrix of residual smoothing. Here, the parameter matrix is typically determined by locally minimizing the residual norm

$$\eta_k^\square = \arg \min \|S_k\| = \arg \min \|S_{k-1} + E_k \eta_k^\square\| = -(E_k^\top E_k)^{-1} (E_k^\top S_{k-1}), \quad (10)$$

where $E_k := R_k - S_{k-1}$ is assumed to have full column rank. Subsequently, the inequality $\|S_k\| \leq \min(\|R_k\|, \|S_{k-1}\|)$ holds, and we obtain a smooth convergence behavior of the residual norms.

There is extensive literature on the relations between residual smoothing and residual gap. For a single right-hand side case, Gutknecht and Rozložník [16] clarified that the conventional smoothing schemes (including the Zhou–Walker implementation) do not help in improving the attainable accuracy. Specifically, rounding errors accumulated in the primary sequences propagate to the smoothed sequences, and the smoothed true residual norms stagnate at the same order of magnitude as the primary ones. To remedy this phenomenon, Komeyama et al. [2, 23] modified the Zhou–Walker implementation to ensure that the primary and smoothed sequences influence one another. This modification is referred to as cross-interactive residual smoothing (CIRS) and can reduce the residual gap and result in a higher attainable accuracy. As SRS has been extended to global and block versions [51, 20], CIRS is also extended. Our previous study [1] presented a global version of CIRS (Gl-CIRS) for the global- and block-type solvers, and therefore, we propose a block version of CIRS (Bl-CIRS) in this study. In contrast to Gl-CIRS, Bl-CIRS requires attention to the conditioning of iteration matrices to be inverted for numerical stability. A common remedy

Table 1: Difference in the recursion formulas for updating smoothed residuals.

Type	SRS scheme	CIRS scheme
Standard ($A\mathbf{x} = \mathbf{b}$)	cf. [37, 49] $\mathbf{s}_k = \mathbf{s}_{k-1} + \eta_k(\mathbf{r}_k - \mathbf{s}_{k-1})$, $\mathbf{r}_k, \mathbf{s}_{k-1} \in \mathbb{R}^n$, $\eta_k \in \mathbb{R}$	cf. [2, 23] $\mathbf{s}_k = \mathbf{s}_{k-1} - \eta_k A\mathbf{v}_k$, $\mathbf{v}_k, \mathbf{s}_{k-1} \in \mathbb{R}^n$, $\eta_k \in \mathbb{R}$
Global ($AX = B$)	cf. [51] $S_k = S_{k-1} + \eta_k(R_k - S_{k-1})$, $R_k, S_{k-1} \in \mathbb{R}^{n \times s}$, $\eta_k \in \mathbb{R}$	cf. [1] $S_k = S_{k-1} - \eta_k AV_k$, $V_k, S_{k-1} \in \mathbb{R}^{n \times s}$, $\eta_k \in \mathbb{R}$
Block ($AX = B$)	cf. [20] $S_k = S_{k-1} + (R_k - S_{k-1})\eta_k^\square$, $R_k, S_{k-1} \in \mathbb{R}^{n \times s}$, $\eta_k^\square \in \mathbb{R}^{s \times s}$	[Present study] $S_k = S_{k-1} - (A\tilde{Q}_k)\tilde{\eta}_k^\square$, $\tilde{Q}_k, S_{k-1} \in \mathbb{R}^{n \times s}$, $\tilde{\eta}_k^\square \in \mathbb{R}^{s \times s}$

is to equivalently reformulate the algorithm to orthonormalize the columns of iteration matrices. BI-CIRS combined with such orthonormalization uses recursion formulas based on the forms (8) to update the approximations and the corresponding smoothed residuals as follows:

$$Y_{k+1} = Y_k + \tilde{Q}_{k+1}\tilde{\eta}_{k+1}^\square, \quad S_{k+1} = S_k - (A\tilde{Q}_{k+1})\tilde{\eta}_{k+1}^\square, \quad k = 0, 1, \dots, \quad (11)$$

where $\tilde{Q}_{k+1} \in \mathbb{R}^{n \times s}$ is a column-orthonormal matrix and $\tilde{\eta}_{k+1}^\square \in \mathbb{R}^{s \times s}$ is a redefined parameter matrix; for details, refer to section 2.2.

Table 1 summarizes the recursion formulas for the aforementioned residual smoothing schemes. This table shows that this study represents a culmination of the CIRS schemes. Since BI-CIRS can be directly derived from the above relationships, our focus is primarily on its theoretical foundation and numerical support. Additionally, we evaluate its residual gap when implemented in conjunction with the orthonormalization strategy.

1.6 Organization

The remainder of this paper is organized as follows. Section 2 describes an underlying BI-CIRS scheme and proposes its refined implementation combined with an orthonormalization strategy. Section 3 conducts numerical experiments to demonstrate the effectiveness of the proposed approach. In section 4, we present a rounding error analysis for the residual gap when using BI-CIRS with the orthonormalization strategy. Finally, concluding remarks are given in section 5.

2 Block cross-interactive residual smoothing

In this section, we present BI-CIRS for reducing the residual gap of the Lanczos-type solvers for (1). All the discussions in this section are assumed to be in exact arithmetic unless otherwise noted.

2.1 Underlying BI-CIRS scheme

We briefly describe an underlying BI-CIRS scheme that is a natural extension of the standard CIRS [2, Algorithm 1] and GI-CIRS [1, Algorithm 3.1] to the block version.

Let $\tilde{P}_k \in \mathbb{R}^{n \times s}$ be the difference $X_{k+1} - X_k$ between adjacent approximations in the primary method. Note that \tilde{P}_k also represents a direction matrix in the recursion formula $X_{k+1} = X_k + \tilde{P}_k$. After generating such a direction matrix \tilde{P}_k , we update an auxiliary matrix V_k recursively as follows:

$$V_{k+1} = V_k(I_s - \eta_k^\square) + \tilde{P}_k,$$

Algorithm 1 Underlying Bl-CIRS scheme.

Require: An initial guess X_0 and the initial residual $R_0 := B - AX_0$.

- 1: Set $Y_0 := X_0$, $S_0 := R_0$, $V_0 := O$, and $\eta_0^\square := O$.
 - 2: **for** $k = 0, 1, 2, \dots$ until convergence **do**
 - 3: Compute \tilde{P}_k (corresponding to $X_{k+1} - X_k$) using the primary method.
 - 4: $V_{k+1} = V_k(I_s - \eta_k^\square) + \tilde{P}_k$
 - 5: Compute $U_{k+1} = AV_{k+1}$ with an explicit multiplication by A .
 - 6: $\eta_{k+1}^\square = (U_{k+1}^\top U_{k+1})^{-1}(U_{k+1}^\top S_k)$
 - 7: $Y_{k+1} = Y_k + V_{k+1}\eta_{k+1}^\square$, $S_{k+1} = S_k - U_{k+1}\eta_{k+1}^\square$
 - 8: **return** $X_{k+1} = Y_{k+1} + V_{k+1}(I_s - \eta_{k+1}^\square)$, $R_{k+1} = S_{k+1} - U_{k+1}(I_s - \eta_{k+1}^\square)$
 - 9: **end for**
-

where $\eta_0^\square := O \in \mathbb{R}^{s \times s}$ and $V_0 := O \in \mathbb{R}^{n \times s}$. Subsequently, explicitly multiplying V_{k+1} by A gives another auxiliary matrix $U_{k+1} := AV_{k+1}$. We next update an approximation and the corresponding smoothed residual by the standard recursion formulas

$$Y_{k+1} = Y_k + V_{k+1}\eta_{k+1}^\square, \quad S_{k+1} = S_k - U_{k+1}\eta_{k+1}^\square,$$

respectively, where $Y_0 := X_0$ and $S_0 := R_0$. Similarly to (10), a local minimization of $\|S_{k+1}\|$ gives $\eta_{k+1}^\square = (U_{k+1}^\top U_{k+1})^{-1}(U_{k+1}^\top S_k)$, where U_{k+1} is assumed to have full column rank. We finally compute the primary approximation and residual by

$$X_{k+1} = Y_{k+1} + V_{k+1}(I_s - \eta_{k+1}^\square), \quad R_{k+1} = S_{k+1} - U_{k+1}(I_s - \eta_{k+1}^\square),$$

and return them to the primary method.

Algorithm 1 displays Bl-CIRS above. By induction, it is shown that Y_k and S_k generated by Algorithm 1 are the same as those generated by (9) with (10). Thus, $\|S_k\| \leq \min(\|R_k\|, \|S_{k-1}\|)$ holds also for Bl-CIRS, and a monotonically decreasing sequence of $\|S_k\|$ can be obtained. The essential difference of Bl-CIRS (Algorithm 1) from Gl-CIRS [1, Algorithm 3.1] (or [2, Algorithm 1]) is that the smoothing parameter of Bl-CIRS is an s -by- s matrix η_k^\square rather than a scalar. For details of CIRS, for instance, its derivation and properties, we refer the reader to [1, 2].

2.2 Orthonormalization strategy

For the numerical stability of Bl-CIRS, we suggest orthonormalizing the columns of the auxiliary matrix $V_k \in \mathbb{R}^{n \times s}$ for each iteration. Hereafter, assume that V_k has full column rank.

Let $V_k = \tilde{Q}_k \tilde{\xi}_k$ be the (thin) QR decomposition, where $\tilde{Q}_k \in \mathbb{R}^{n \times s}$ is a column-orthonormal matrix and $\tilde{\xi}_k \in \mathbb{R}^{s \times s}$ is the associated upper triangular matrix. Then, introducing auxiliary matrices $\tilde{U}_k := A\tilde{Q}_k$ and $\tilde{\eta}_k^\square := \tilde{\xi}_k \eta_k^\square$, the approximations and residuals in Algorithm 1 are rewritten as

$$\begin{aligned} Y_k &= Y_{k-1} + V_k \eta_k^\square = Y_{k-1} + \tilde{Q}_k \tilde{\eta}_k^\square, \\ S_k &= S_{k-1} - U_k \eta_k^\square = S_{k-1} - \tilde{U}_k \tilde{\eta}_k^\square, \\ X_k &= Y_k + V_k(I_s - \eta_k^\square) = Y_k + \tilde{Q}_k(\tilde{\xi}_k - \tilde{\eta}_k^\square), \\ R_k &= S_k - U_k(I_s - \eta_k^\square) = S_k - \tilde{U}_k(\tilde{\xi}_k - \tilde{\eta}_k^\square), \end{aligned}$$

where the quantity $\tilde{U}_k := A\tilde{Q}_k (= (S_{k-1} - R_k)\tilde{\xi}_k^{-1})$ is given by explicitly multiplying \tilde{Q}_k by A instead of $U_k := AV_k (= S_{k-1} - R_k)$. Similarly, the next auxiliary matrix can be expressed by

$$(\tilde{Q}_{k+1}\tilde{\xi}_{k+1} =) V_{k+1} = V_k(I_s - \eta_k^\square) + \tilde{P}_k = \tilde{Q}_k(\tilde{\xi}_k - \tilde{\eta}_k^\square) + \tilde{P}_k.$$

The redefined smoothing parameter $\tilde{\eta}_k^\square$ is computed by

$$\begin{aligned} \tilde{\eta}_k^\square &:= \tilde{\xi}_k \eta_k^\square = \tilde{\xi}_k (U_k^\top U_k)^{-1} (U_k^\top S_{k-1}) \\ &= [(U_k \tilde{\xi}_k^{-1})^\top U_k \tilde{\xi}_k^{-1}]^{-1} [(U_k \tilde{\xi}_k^{-1})^\top S_{k-1}] = (\tilde{U}_k^\top \tilde{U}_k)^{-1} (\tilde{U}_k^\top S_{k-1}), \end{aligned}$$

Algorithm 2 Refined BI-CIRS scheme with orthonormalization.

Require: An initial guess X_0 and the initial residual $R_0 := B - AX_0$.

- 1: Set $Y_0 := X_0$, $S_0 := R_0$, $\tilde{Q}_0 := O$, $\tilde{\xi}_0 := O$, and $\tilde{\eta}_0^\square := O$.
 - 2: **for** $k = 0, 1, 2, \dots$ until convergence **do**
 - 3: Compute \tilde{P}_k (corresponding to $X_{k+1} - X_k$) using the primary method.
 - 4: $V_{k+1} = \tilde{Q}_k(\tilde{\xi}_k - \tilde{\eta}_k^\square) + \tilde{P}_k$
 - 5: Compute QR decomposition: $[\tilde{Q}_{k+1}, \tilde{\xi}_{k+1}] = \mathbf{qr}(V_{k+1})$.
 - 6: Compute $\tilde{U}_{k+1} = A\tilde{Q}_{k+1}$ with an explicit multiplication by A .
 - 7: $\tilde{\eta}_{k+1}^\square = (\tilde{U}_{k+1}^\top \tilde{U}_{k+1})^{-1}(\tilde{U}_{k+1}^\top S_k)$
 - 8: $Y_{k+1} = Y_k + \tilde{Q}_{k+1}\tilde{\eta}_{k+1}^\square$, $S_{k+1} = S_k - \tilde{U}_{k+1}\tilde{\eta}_{k+1}^\square$
 - 9: **return** $X_{k+1} = Y_{k+1} + \tilde{Q}_{k+1}(\tilde{\xi}_{k+1} - \tilde{\eta}_{k+1}^\square)$, $R_{k+1} = S_{k+1} - \tilde{U}_{k+1}(\tilde{\xi}_{k+1} - \tilde{\eta}_{k+1}^\square)$
 - 10: **end for**
-

or equivalently, the final term comes from a local minimization of the smoothed residual norm, i.e., $\tilde{\eta}_k^\square = \arg \min \|S_{k-1} - \tilde{U}_k \tilde{\eta}_k^\square\|$. Here, the condition number of \tilde{U}_k is bounded above by that of A .

Algorithm 2 displays BI-CIRS combined with the orthonormalization strategy. Here, $[\cdot, \cdot] = \mathbf{qr}(\cdot)$ denotes the QR decomposition of a matrix in parentheses; the first and second variables on the left-hand side are the Q- and R-factors, respectively. The approximations and corresponding smoothed residuals are updated by the forms (11), and these forms are crucial in reducing the residual gap; refer to the next section and section 3.2.

2.3 Effect of approximation norms on the residual gap

The residual gap G_{R_k} (6) in Theorem 1.1 reduces to

$$\|G_{R_k}\| < c_x \|A\| \max_{0 < j \leq k} \|X_j\| + c_r \max_{0 \leq j \leq k} \|R_j\|, \quad (12)$$

where the coefficients c_x and c_r are small positive scalars of order \mathbf{u} (see also the analysis in section 4 and [15, 16]). Because BI-CIRS with the orthonormalization strategy uses the recursion formulas (11) that are essentially the same as (8), the bound (12) also holds for the smoothed case; that is, X_j , R_j , and G_{R_k} are replaced by Y_j , S_j , and $G_{S_k} := (B - AY_k) - S_k$, respectively. Note that $\|S_j\|$ decreases monotonically, whereas $\|R_j\|$ can oscillate significantly. The residual gap can be suppressed by suppressing $\max_j \|R_j\|$ in the second term in (12). However, the bound also depends on $\max_j \|X_j\|$. Therefore, we discuss the effect of the residual smoothing on the convergence behavior of the approximation norms.

From the recursion formula $Y_{k+1} = Y_k + \tilde{Q}_{k+1}\tilde{\eta}_{k+1}^\square$, the norm of the updated approximation is bounded as follows:

$$\|Y_k\| - \|\tilde{\eta}_{k+1}^\square\| \leq \|Y_{k+1}\| \leq \|Y_k\| + \|\tilde{\eta}_{k+1}^\square\|. \quad (13)$$

As $\|S_{k+1}\| \leq \|S_k\|$ holds, we have

$$\|\tilde{\eta}_{k+1}^\square\| = \|A^{-1}(S_k - S_{k+1})\| \leq 2\|A^{-1}\|\|S_k\|,$$

and the above bounds lead to the following inequalities:

$$\frac{\|Y_k\|}{\|B\|} - 2\tau_k \leq \frac{\|Y_{k+1}\|}{\|B\|} \leq \frac{\|Y_k\|}{\|B\|} + 2\tau_k, \quad \tau_k := \|A^{-1}\| \frac{\|S_k\|}{\|B\|}.$$

Here, $\|S_k\|/\|B\|$ (≤ 1 for $Y_0 := O$) decreases monotonically with increasing k . Therefore, if $\|A^{-1}\|$ is modest, then the difference between $\|Y_k\|$ and $\|Y_{k+1}\|$ is also modest and becomes smaller as the iteration proceeds. Even at the early stage of iterations, because $\|\tilde{\eta}_k^\square\|$ is small for a large $\|R_k\|$ from (9), there may be no large oscillations in $\|Y_k\|$ from (13). Thus, the sequence of the

approximation norms starting with $\|Y_0\| = 0$ can have a smooth (not necessarily monotonic) convergence behavior in the generic case.

However, from the equality $Y_k = X^* - A^{-1}S_k$ for $X^* := A^{-1}B$, an upper bound of the approximation norms is given as follows:

$$\frac{\|Y_k\|}{\|B\|} \leq \frac{\|X^*\|}{\|B\|} + \tau_k.$$

Therefore, we expect that $\|Y_k\|$ will remain small relative to $\|X^*\|$. In the methods without residual smoothing, S_k is replaced by R_k in the definition of τ_k , and the upper bound of $\|X_k\|$ can be magnified by the oscillations in $\|R_k\|$.

In actual computation, as will be shown in section 3.2.2, $\|Y_k\|$ increases smoothly and approaches $\|X^*\|$, whereas $\|X_k\|$ can oscillate significantly during the iterations. This is a strength of the residual smoothing from the perspective of the approximation norms and contributes to preventing a large residual gap.

2.4 Specific Lanczos-type solver with BI-CIRS

We present a specific Lanczos-type solver combined with the proposed BI-CIRS with the orthonormalization strategy. We apply Algorithm 2 to the BI-BiCGSTABpQ method, which is a stabilized variant of the well-established method BI-BiCGSTAB and orthonormalizes the columns of iteration matrices [10, 28]. Our derivation below follows those of the smoothed GI- and BI-BiCGSTABpQ combined with GI-CIRS [1, sections 5.2 and 5.3]; the resulting algorithm is an extension of [1, Algorithm 5.3] for using BI-CIRS.

As noted in [1], BI-BiCGSTABpQ updates the approximation X_k and the corresponding residual R_k by two steps at each iteration as follows:

$$\begin{aligned} \text{(BiCG part)} \quad X'_k &:= X_k + Q_k \alpha_k^\square, & R'_k &:= R_k - (AQ_k) \alpha_k^\square, \\ \text{(polynomial part)} \quad X_{k+1} &= X'_k + \omega_k R'_k, & R_{k+1} &= R'_k - \omega_k (AR'_k), \end{aligned} \tag{14}$$

where $\omega_k \in \mathbb{R}$ is normally determined by minimizing $\|R_{k+1}\|$ and $Q_k \in \mathbb{R}^{n \times s}$ (a column-orthonormalized matrix) is the Q-factor of the QR decomposition of the direction matrix; see below for $\alpha_k^\square \in \mathbb{R}^{s \times s}$. It is simple to apply BI-CIRS to both the residuals in the BiCG and polynomial parts, but this approach requires two additional multiplications by A per iteration. Therefore, following the concept in [1, 2], we apply BI-CIRS only to the BiCG part residuals to reduce the computational costs. Specifically, we reformulate (14) as follows:

$$X'_k = X'_{k-1} + \tilde{P}_{k-1}, \quad R'_k = R'_{k-1} - A\tilde{P}_{k-1}, \quad \tilde{P}_{k-1} := \omega_{k-1} R'_{k-1} + Q_k \alpha_k^\square,$$

and apply Algorithm 2 to the primary sequences $\{X'_k\}$ and $\{R'_k\}$, where $X'_{-1} := X_0$, $R'_{-1} := O$, and $\omega_{-1} := 0$. The setting of \tilde{P}_k is variable depending on the primary sequence to which BI-CIRS is applied. Moreover, to reduce the number of multiplications by A , we obtain α_k^\square as a solution of an s -dimensional linear system $(Z_0^\bullet \top Q_k) \alpha_k^\square = R_0^\bullet \top R_k$, where $Z_0^\bullet := A^\top R_0^\bullet$ is computed once and stored in advance. Although AQ_k is needed to compute the next direction matrix, it can be provided by solving the system $(AQ_k) \alpha_k^\square = R_k - R'_k$, after R'_k is returned from BI-CIRS. The resulting algorithm requires no additional multiplications by A .

Algorithm 3 displays the smoothed BI-BiCGSTABpQ using BI-CIRS with the orthonormalization strategy. In line 6, $\mathbf{qf}(\cdot)$ denotes the Q-factor of the QR decomposition of a matrix. This algorithm requires two orthonormalizations per iteration; one is for the direction matrix P_k in BI-BiCGSTABpQ and another is for the auxiliary matrix V_k in BI-CIRS. Lines 8–12 correspond to BI-CIRS, where $\tilde{\zeta}_k := \tilde{\xi}_k - \tilde{\eta}_k^\square$ is introduced for efficiency. The indices of variables (e.g., the number of iterations k) are omitted in the actual implementation: however, several variables that can be overwritten by others remain for clarity and readability. For instance, the storage for n -by- s matrices can be reduced by overwriting the orthonormalized matrices Q and \tilde{Q} with P and V , respectively. Moreover, we do not need to compute X and X' if satisfied with Y to capture approximations for (1).

Algorithm 3 Smoothed BI-BiCGSTABpQ using BI-CIRS with orthonormalization.

- 1: Select an initial guess X and compute the initial residual $R = B - AX$.
 - 2: Set $Y := X$, $S := R$, $\tilde{Q} := O$, and $\tilde{\zeta} := O$.
 - 3: Select an initial shadow residual R_0^\bullet and compute $Z_0^\bullet = A^\top R_0^\bullet$.
 - 4: Set $P := R$, $R' := O$, and $\omega := 0$.
 - 5: **while** $\|S\| > tol$ **do**
 - 6: $Q = \mathbf{qf}(P)$, $\sigma = Z_0^{\bullet\top} Q$
 - 7: Solve $\sigma\alpha = R_0^{\bullet\top} R$ for α .
 - 8: $\tilde{P} = \omega R' + Q\alpha$, $V = \tilde{Q}\tilde{\zeta} + \tilde{P}$
 - 9: $[\tilde{Q}, \tilde{\xi}] = \mathbf{qr}(V)$, $\tilde{U} = A\tilde{Q}$
 - 10: Solve $(\tilde{U}^\top \tilde{U})\tilde{\eta} = \tilde{U}^\top \tilde{S}$ for $\tilde{\eta}$.
 - 11: $Y = Y + \tilde{Q}\tilde{\eta}$, $S = S - \tilde{U}\tilde{\eta}$, $\tilde{\zeta} = \tilde{\xi} - \tilde{\eta}$
 - 12: $X' = Y + \tilde{Q}\tilde{\zeta}$, $R' = S - \tilde{U}\tilde{\zeta}$
 - 13: Solve $V'\alpha = R - R'$ for V' .
 - 14: $T = AR'$, $\omega = \langle R', T \rangle_F / \langle T, T \rangle_F$
 - 15: $X = X' + \omega R'$, $R = R' - \omega T$
 - 16: Solve $\sigma\beta = R_0^{\bullet\top} T$ for β .
 - 17: $P = R - (Q - \omega V')\beta$
 - 18: **end while**
-

3 Numerical experiments

In this section, numerical experiments demonstrate that Algorithm 3 can effectively reduce the residual gap and improve the attainable accuracy of the approximations. We first describe common settings of the experiments, and then show the numerical results, dividing them into several viewpoints.

3.1 Computational conditions

Numerical calculations were conducted by double-precision floating-point arithmetic on a PC (Intel Core i7-1185G7 CPU with 32 GB of RAM) equipped with MATLAB R2021a.

The iterations were started with $X_0 := O$ and were stopped when the relative residual norms (i.e., $\|S_k\|/\|B\|$ and $\|R_k\|/\|B\|$ for the methods with and without residual smoothing, respectively) were less than 10^{-15} . The maximum number of iterations was set to n . Following [1], the test matrices A were given from the SuiteSparse Matrix Collection [7]. Table 2 displays the dimension (n), number of nonzero entries (nnz), maximum number of nonzero entries per row (m), and 2-norm condition number ($\text{cond}_2(A)$). The right-hand side B was given by a random matrix with setting $s = 16, 32$, and the initial shadow residual R_0^\bullet was set to $R_0 (= B)$.

We used BI-BiCGSTABpQ as an underlying solver and compared its five variations listed below.

Solver 1: No residual smoothing (the simple BI-BiCGSTABpQ).

Solver 2: Using BI-SRS ((9) with (10)).

Solver 3: Using BI-CIRS without orthonormalization (Algorithm 1).

Solver 4: Using BI-CIRS with orthonormalization (Algorithm 2).

Solver 5: Using GI-CIRS ([1, Algorithm 5.3]).

Note that Solver 4 is our proposed method and corresponds to Algorithm 3. In the implementation on MATLAB, the slash or backslash command was used for solving the small linear systems (e.g., lines 7, 10, 13, and 16 in Algorithm 3), and the QR decomposition used in the solvers was performed by the $\mathbf{qr}(\cdot)$ command. All the solvers require two multiplications by A per iteration.

Table 2: Characteristics of test matrices [7].

Matrix	n	nnz	m	$\text{cond}_2(A)$
cdde2	961	4,681	5	5.48e+01
pde2961	2,961	14,585	5	6.42e+02
bfwa782	782	7,514	24	1.74e+03

Table 3: Number of iterations, computation time, and true relative residual norm of Solvers 1–5 for test matrices.

Matrix	Solver	$s = 16$			$s = 32$		
		Iter.	Time (s)	True res.	Iter.	Time (s)	True res.
cdde2	#1	55	0.026	1.58e−13	39	0.038	6.91e−11
	#2	54	0.028	2.29e−13	38	0.045	6.91e−11
	#3	55	0.042	2.83e−13	39	0.054	4.00e−11
	#4	55	0.046	7.78e−15	38	0.059	6.71e−15
	#5	56	0.038	7.41e−15	39	0.050	6.13e−15
pde2961	#1	96	0.116	9.72e−11	64	0.174	5.05e−13
	#2	94	0.124	1.09e−10	62	0.180	7.20e−11
	#3	100	0.157	7.77e−11	883	3.298	2.21e−11
	#4	93	0.156	6.53e−14	60	0.243	5.33e−14
	#5	90	0.119	6.19e−14	65	0.204	5.21e−14
bfwa782	#1	61	0.029	1.21e−12	40	0.036	1.64e−12
	#2	61	0.033	7.44e−11	37	0.037	4.26e−11
	#3	†	-	4.85e−11	†	-	2.47e−11
	#4	62	0.042	7.69e−14	36	0.051	6.41e−14
	#5	62	0.037	7.44e−14	38	0.046	6.10e−14

3.2 Effectiveness of the orthonormalization strategy

Here, we present the numerical results of Solvers 1–5 applied to (1). Table 3 displays the number of iterations (**Iter.**), computation time (**Time (s)**), and true relative residual norm (**True res.**) at the termination of the iterations, where the true relative residual norm was evaluated by $\|B - AX_k\|/\|B\|$ and $\|B - AY_k\|/\|B\|$ for Solver 1 and Solvers 2–5, respectively. The symbol † denotes no convergence within n iterations.

We observe from Table 3 that the solvers, except for Solver 3, converge at a similar speed for each matrix, but Solvers 4 and 5 generate more accurate approximations than the others with respect to the true relative residual norm. The computation time is only a guide because the provided algorithms were implemented naively on MATLAB, and their efficiencies depend on the computational equipment and implementation. We will not discuss this point further. In the following, we focus on the residual gap and discuss the feature of BI-CIRS for each comparison item.

3.2.1 Comparison of the residual gap

We first compare the convergence behaviors of the residual norms for Solvers 1–4. Figure 1 shows the histories of the relative norms of the recursively updated and true residuals of Solvers 1–4 for cdde2 with $s = 32$. The plots indicate the number of iterations on the horizontal axis versus \log_{10} of the relative residual norm on the vertical axis.

From Figure 1, we observe the following. As noted in [1], Solver 1 (i.e., the original BI-BiCGSTABpQ) has a large peak of the residual norms, leading to a large residual gap; that is, the

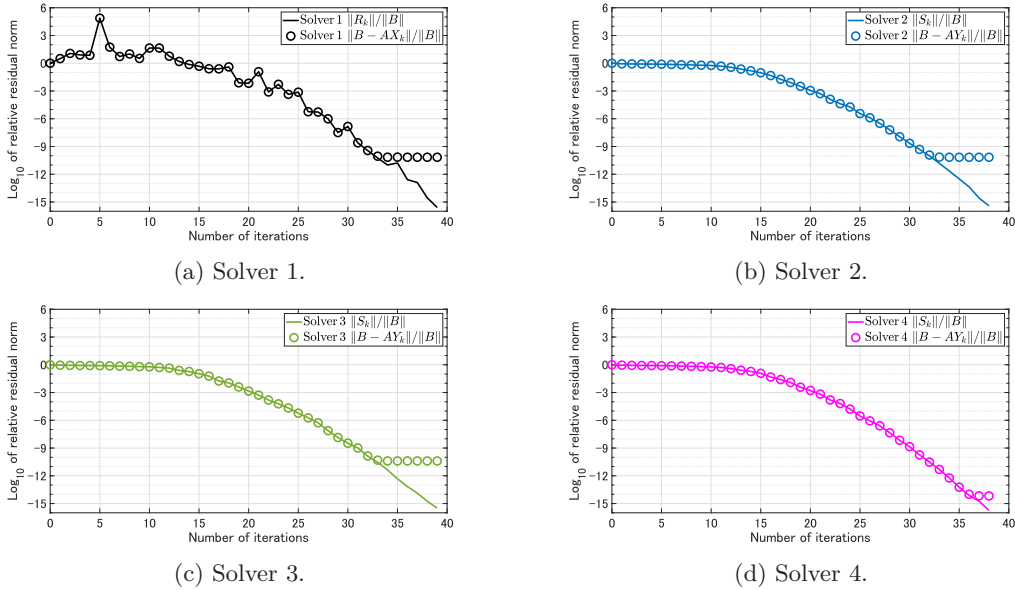


Figure 1: Convergence histories of Solvers 1–4 for cdde2 with $s = 32$.

true residual norms stagnate at a certain level of accuracy while the recursively updated residual norms approach zero. Solvers 2–4 (i.e., the methods with residual smoothing) have a smooth convergence behavior. However, Solvers 2 and 3 have still a large residual gap and their true residual norms stagnate at the same order of magnitude as Solver 1, whereas only Solver 4 has a smaller residual gap and generates more accurate approximations regarding the true residual norm. In addition, Solver 3 (using BI-CIRS without the orthonormalization) has numerical stability problems such that the convergence often deteriorates as shown in Table 3. These results suggest that orthonormalization is crucial in stabilizing BI-CIRS and in avoiding the increase of the residual gap. Similar observations were obtained as well for other matrices and several right-hand sides.

3.2.2 Convergence behavior of approximation norms

Furthermore, we examine the convergence behavior of the approximation norms with and without residual smoothing. In particular, we present examples in which $\max_j \|R_j\| \leq \max_j \|X_j\|$ holds and discuss the influence of the approximation norms on the residual gap.

Figures 2 and 3 show the convergence histories of the relative residual and approximation norms of Solvers 1 and 4 for pde2961 and bwf782, respectively, where $s = 16$. To see the oscillations in the residual and approximation norms precisely, the number of matrix-matrix multiplications (MMs) with A is plotted on the horizontal axis, and we illustrate the norms corresponding to the Bi-CG and polynomial parts alternately for Solver 1 (cf. (14)). The attainable accuracy, that is, the final size of the true relative residual norms at termination, is indicated with a dashed line with the same color as the corresponding residual norms.

From Figures 2 and 3, we observe the following: Solver 4 has a smooth convergence behavior with respect to the residual norms $\|S_k\|$ but approximation norms $\|Y_k\|$, whereas Solver 1 exhibits the oscillations in $\|X_k\|$ along with $\|R_k\|$. As described in Figure 2, the loss of attainable accuracy seems to be determined by the maximum value of the approximation norms; for instance, the final accuracy $\|B - AX_k\|/\|B\| = 9.72 \times 10^{-11}$ at termination of Solver 1 corresponds to the order of $\max_j \|X_j\|/\|B\| \times 10^{-15}$ ($= 9.03 \times 10^4 \times 10^{-15}$). This result follows the residual gap evaluation (12). In Solver 4, because it holds that $\max_j \|S_j\|/\|B\| = \|S_0\|/\|B\| = 1$ for $Y_0 := O$, the size of $\|Y_k\|$ directly affects the residual gap. Although $\|Y_k\|$ is not necessarily increasing monotonically as described in Figure 3, it mostly behaves smoothly and the maximum value is almost the same order of magnitude as $\|X^*\|$. These observations follow the discussions in section 2.3. Thus, we

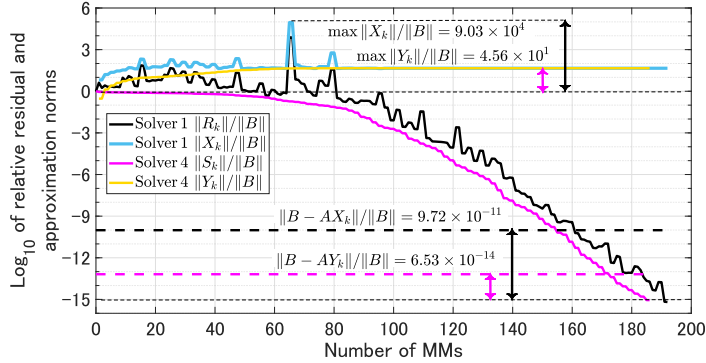


Figure 2: Convergence histories of the relative residual and approximation norms of Solvers 1 and 4 for pde2961 with $s = 16$.

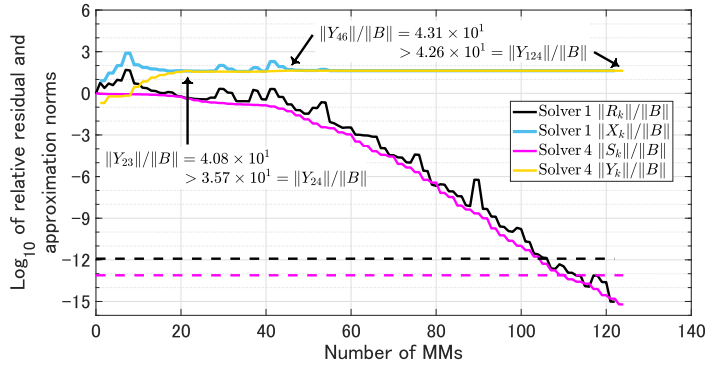


Figure 3: Convergence histories of the relative residual and approximation norms of Solvers 1 and 4 for bfw782 with $s = 16$.

conclude that BI-CIRS effectively suppresses the residual gap via the residual and approximation norm.

3.2.3 Comparison between BI-CIRS and GI-CIRS

We finally compare the convergence behaviors of Solvers 4 and 5 to investigate the difference between BI-CIRS and GI-CIRS. Figure 4 shows the convergence histories of the relative residual norms of Solvers 4 and 5 for all the combinations of the test matrices and the number of s . The number of iterations and \log_{10} of the relative residual norm are plotted on the horizontal and vertical axes, respectively.

From Table 3 and Figure 4, we observe the following. The residual gaps of Solvers 4 and 5 are sufficiently small and their approximations attain the same level of accuracy. However, Solver 4 exhibits even smoother convergence behavior than Solver 5, and the convergence speed of Solver 4 is slightly faster in several cases. Figure 4c shows that Solver 4 does not always offer smaller residual norms than Solver 5.

As seen in the comparisons between the global- and block-type solvers, GI-CIRS and BI-CIRS have their strengths. For instance, GI-CIRS requires smaller computational costs per iteration than BI-CIRS, but BI-CIRS could be more efficient in parallel. BI-CIRS excels in smoothing residual norms as shown above, while GI-CIRS would be easier to apply to more general matrix equations (cf. [1]). Therefore, it is difficult to state which between GI-CIRS and BI-CIRS is better.

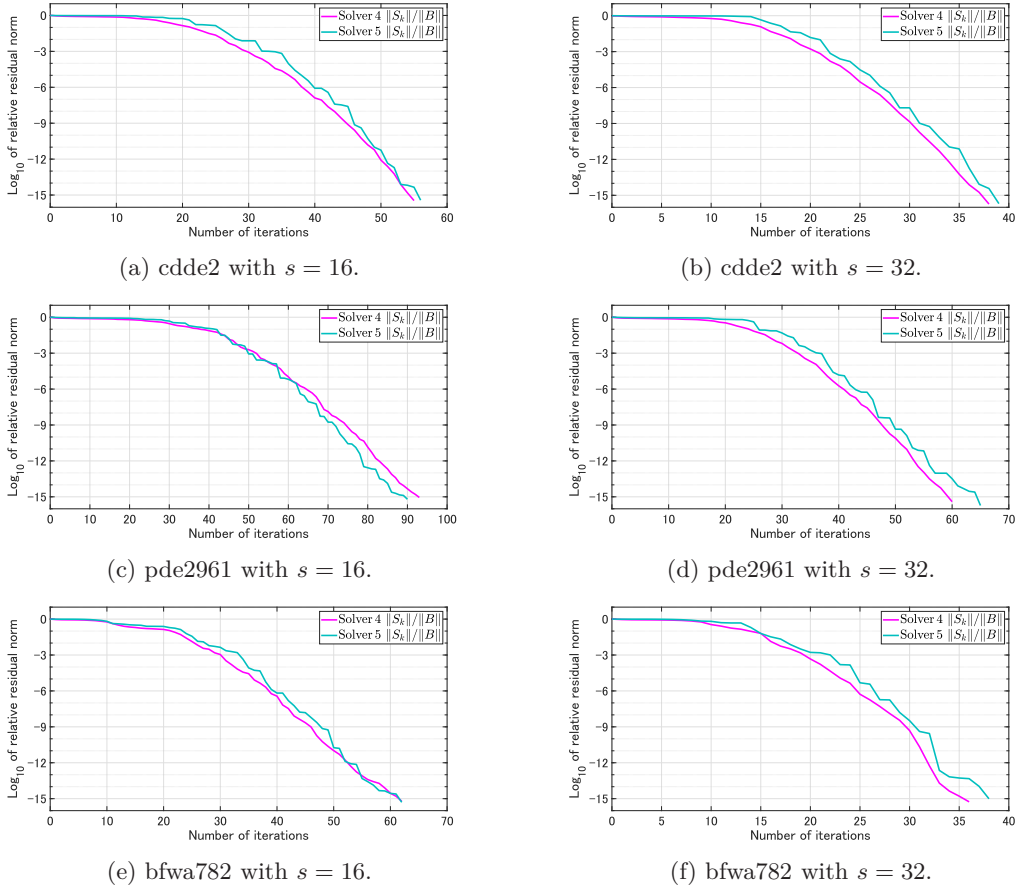


Figure 4: Convergence histories of Solvers 4 and 5 for test matrices.

4 Rounding error analysis for the residual gap

In this section, a detailed rounding error analysis shows that BI-CIRS with the orthonormalization strategy suppresses the residual gap. The new results evaluate the residual gap fully in finite precision arithmetic and complement the results in [1] when using backward stable orthonormalization processes; Givens rotations and Householder transformations. A more general case is also presented in Appendix A.

We first describe our main result on the residual gap; the proof will be presented in section 4.3.

Theorem 4.1. *In finite precision arithmetic, let $X_k \in \mathbb{F}^{n \times s}$ and $R_k \in \mathbb{F}^{n \times s}$ be the k th approximation and residual, respectively, generated by the recursion formulas*

$$X_k = X_{k-1} + \widehat{Q}_{k-1} \alpha_{k-1}^\square, \quad R_k = R_{k-1} - (A \widehat{Q}_{k-1}) \alpha_{k-1}^\square, \quad (15)$$

where \widehat{Q}_{k-1} is a Q -factor of the direction matrix P_{k-1} obtained from the QR decomposition with Givens rotations or Householder transformations. Then, with $X_0 = O$, the norm of the residual gap $G_{R_k} := (B - AX_k) - R_k$ is bounded as follows:

$$\|G_{R_k}\| < (8\sqrt{s}\gamma_{m+3s} + \gamma_1) k \|A\| \max_{0 < i \leq k} \|X_i\| + k\gamma_1 \max_{0 < i \leq k} \|R_i\|. \quad (16)$$

Here, we refer to the subsections below for the values of γ and the related assumptions.

This theorem shows that we must avoid large peaks of the approximation and residual norms to suppress the increase of the residual gap. For BI-CIRS, replacing X_k and R_k by Y_k and S_k ,

respectively, in (15), Theorem 4.1 holds for the residual gap $G_{S_k} := (B - AY_k) - S_k$. Therefore, as indicated right after [1, Corollary 2.3], even when using an inexact orthonormalization, Bl-CIRS smoothes the convergence of the residual and approximation norms and can reduce the residual gap. This theoretical result is consistent with the numerical results in section 3.

To prove Theorem 4.1, we exploit rounding error models in [17] and evaluate local error bounds for (15).

4.1 Error models for matrix computations

Our analysis is based on the following models for matrix operations in finite precision arithmetic [17]:

$$\mathfrak{fl}(P + Q) = P + Q + E', \quad \|E'\| \leq \mathbf{u}\|P + Q\|, \quad (17)$$

$$\mathfrak{fl}(P\alpha^\square) = P\alpha^\square + E^\square, \quad \|E^\square\| \leq \gamma_s \|P\| \|\alpha^\square\|, \quad (18)$$

$$\mathfrak{fl}(AP) = AP + E''', \quad \|E''' \| \leq \gamma_m \|A\| \|P\| \quad (19)$$

for given $P, Q \in \mathbb{F}^{n \times s}$ and $\alpha^\square \in \mathbb{F}^{s \times s}$, where γ_k is defined by

$$\gamma_k := \frac{k\mathbf{u}}{1 - k\mathbf{u}},$$

and an assumption $k\mathbf{u} < 1$ is implicitly imposed whenever we use γ_k . For the notations \mathbb{F} , $\mathfrak{fl}(\cdot)$, \mathbf{u} , and m , we refer the reader to the sentence right before Theorem 1.1. In the following, we focus on using Givens rotation and Householder transformation to orthonormalize the columns of $P_{k-1} \in \mathbb{R}^{n \times s}$ and introduce their known rounding error bounds.

The QR decomposition of $P_{k-1} \in \mathbb{R}^{n \times s}$ using Given rotations [17, section 19.6] or Householder transformations [17, section 19.3] numerically computes a Q-factor $\widehat{Q}_{k-1}^{\text{full}} = \begin{bmatrix} \widehat{Q}_{k-1} & \widehat{Q}'_{k-1} \end{bmatrix} \in \mathbb{R}^{n \times n}$ with $\widehat{Q}_{k-1} \in \mathbb{R}^{n \times s}$ such that

$$\begin{aligned} \widehat{Q}_{k-1} &= Q_{k-1} \left(\begin{bmatrix} I_s \\ O \end{bmatrix} + \Delta I_{k-1} \right), \quad \Delta I_{k-1} \in \mathbb{R}^{n \times s}, \\ \|\Delta I_{k-1}(:, j)\|_2 &\leq \begin{cases} \tilde{\gamma}_{n+s-2} & \text{for Givens,} \\ \tilde{\gamma}_{ns} & \text{for Householder,} \end{cases} \end{aligned} \quad (20)$$

for $j = 1, 2, \dots, s$, where $Q_{k-1} \in \mathbb{R}^{n \times n}$ is the product of Givens rotations or Householder transformations and is the Q-factor (an exactly orthogonal matrix) of the full QR decomposition of P_{k-1} and $\|\cdot\|_2$ denotes the Euclidean norm. Here, the notation $X(:, j)$ follows the MATLAB convention, that is, it stands for the j th column of the matrix X . The scalar $\tilde{\gamma}_k$ is defined by

$$\tilde{\gamma}_k = \frac{ck\mathbf{u}}{1 - ck\mathbf{u}},$$

where c is a small integer constant greater than one [17, eq. (3.8)], and $ck\mathbf{u} < 1$ is assumed similarly to γ_k . From (20), it holds that

$$\left\| \widehat{Q}_{k-1} \right\| \leq \|I_s\| + \|\Delta I_{k-1}\| \leq \begin{cases} \sqrt{s}(1 + \tilde{\gamma}_{n+s-2}) & \text{for Givens,} \\ \sqrt{s}(1 + \tilde{\gamma}_{ns}) & \text{for Householder.} \end{cases}$$

In the analysis below, we will use the bounds

$$\tilde{\gamma}_j + \tilde{\gamma}_k + \tilde{\gamma}_j \tilde{\gamma}_k < \tilde{\gamma}_{j+k} \quad \text{for } c(j+k)\mathbf{u} < 1, \quad (21)$$

$$\gamma_k < \tilde{\gamma}_k \quad \text{for } ck\mathbf{u} < 1, \quad (22)$$

$$\gamma_j \tilde{\gamma}_k < \min(\gamma_j, \tilde{\gamma}_k) \leq \max(\gamma_j, \tilde{\gamma}_k) \quad \text{for } \max(j, k)c\mathbf{u} < 1/2 \quad (23)$$

for positive integers j and k , and a constant c ; see also [17, Lemma 3.3].

4.2 Local errors in recursion formulas

Here, we analyze local errors when using the recursion formulas (15). The local errors E_{X_k} and E_{R_k} in the updated approximation and residual, respectively, can be expressed as follows:

$$\begin{aligned} X_k &= \text{fl}(X_{k-1} + \text{fl}(\widehat{Q}_{k-1}\alpha_{k-1}^\square)) \\ &= X_{k-1} + \text{fl}(\widehat{Q}_{k-1}\alpha_{k-1}^\square) + E'_{X_k} \end{aligned} \quad (24)$$

$$\begin{aligned} &= X_{k-1} + \widehat{Q}_{k-1}\alpha_{k-1}^\square + E'_{X_k} + E_{X_k}^\square \\ &= X_{k-1} + \widehat{Q}_{k-1}\alpha_{k-1}^\square + E_{X_k}, \end{aligned} \quad (25)$$

where $E_{X_k} := E'_{X_k} + E_{X_k}^\square$, and

$$\begin{aligned} R_k &= \text{fl}(R_{k-1} - \text{fl}(\text{fl}(A\widehat{Q}_{k-1})\alpha_{k-1}^\square)) \\ &= R_{k-1} - \text{fl}(\text{fl}(A\widehat{Q}_{k-1})\alpha_{k-1}^\square) - E'_{R_k} \\ &= R_{k-1} - \text{fl}(A\widehat{Q}_{k-1})\alpha_{k-1}^\square - E'_{R_k} - E_{R_k}^\square \\ &= R_{k-1} - A\widehat{Q}_{k-1}\alpha_{k-1}^\square - E'_{R_k} - E_{R_k}^\square - E_{R_k}''' \alpha_{k-1}^\square \\ &= R_{k-1} - A\widehat{Q}_{k-1}\alpha_{k-1}^\square - E_{R_k}, \end{aligned}$$

where $E_{R_k} := E'_{R_k} + E_{R_k}^\square + E_{R_k}''' \alpha_{k-1}^\square$. Subsequently, the local errors satisfy the bounds below.

Lemma 4.1. *For (15) in finite precision arithmetic, assume that \widehat{Q}_{k-1} is a numerically computed Q -factor of the QR decomposition of P_{k-1} using Givens rotations or Householder transformations, and that c , n , s , and \mathbf{u} satisfy*

$$\begin{cases} c[(n+2(s-1))(\sqrt{s}+1)+1]\mathbf{u} < \frac{1}{2} & \text{for Givens,} \\ c[(n+1)(\sqrt{s}+1)s+1]\mathbf{u} < \frac{1}{2} & \text{for Householder.} \end{cases} \quad (26)$$

Then, for $k \geq 1$, the local errors are bounded as follows:

$$\|E_{X_k}\| < 4\sqrt{s}\gamma_s(\|X_{k-1}\| + \|X_k\|) + \gamma_1\|X_k\|, \quad (27)$$

$$\|E_{R_k}\| < \gamma_1\|R_k\| + 4\sqrt{s}(\gamma_m + 2\gamma_s)\|A\|(\|X_{k-1}\| + \|X_k\|). \quad (28)$$

Proof. The assumptions imply that $c(n+s-2)\mathbf{u} < 1$ and $cn_s\mathbf{u} < 1$ hold and ensure the existence of \widehat{Q}_{k-1} such that (20) is satisfied.

From (17), it follows that

$$\|E'_{X_k}\| \leq \mathbf{u}\|X_{k-1} + \text{fl}(\widehat{Q}_{k-1}\alpha_{k-1}^\square)\| \leq \mathbf{u}(\|X_k\| + \|E'_{X_k}\|),$$

in which the last inequality is from (24), that is, $X_{k-1} + \text{fl}(\widehat{Q}_{k-1}\alpha_{k-1}^\square) = X_k - E'_{X_k}$. Subsequently, we obtain the bound

$$\|E'_{X_k}\| \leq \gamma_1\|X_k\|. \quad (29)$$

Next, it follows from (18) that

$$\|E_{X_k}^\square\| \leq \gamma_s\|\widehat{Q}_{k-1}\|\|\alpha_{k-1}^\square\| \leq \begin{cases} \sqrt{s}(1 + \tilde{\gamma}_{n+s-2})\gamma_s\|\alpha_{k-1}^\square\| & \text{for Givens,} \\ \sqrt{s}(1 + \tilde{\gamma}_{ns})\gamma_s\|\alpha_{k-1}^\square\| & \text{for Householder.} \end{cases} \quad (30)$$

Combining these bounds with (25) and (29) gives

$$\begin{aligned} \|\widehat{Q}_{k-1}\alpha_{k-1}^\square\| &\leq \|X_{k-1}\| + \|X_k\| + \|E'_{X_k}\| + \|E_{X_k}^\square\| \\ &\leq \begin{cases} \|X_{k-1}\| + (1 + \gamma_1)\|X_k\| + \sqrt{s}(1 + \tilde{\gamma}_{n+s-2})\gamma_s\|\alpha_{k-1}^\square\| & \text{for Givens,} \\ \|X_{k-1}\| + (1 + \gamma_1)\|X_k\| + \sqrt{s}(1 + \tilde{\gamma}_{ns})\gamma_s\|\alpha_{k-1}^\square\| & \text{for Householder.} \end{cases} \end{aligned}$$

Regarding α_{k-1}^\square , we have

$$\begin{aligned}\|\alpha_{k-1}^\square\| &= \|Q_{k-1}(\cdot, 1:s) \alpha_{k-1}^\square\| \\ &= \left\| \left(\widehat{Q}_{k-1} - Q_{k-1} \Delta I_{k-1} \right) \alpha_{k-1}^\square \right\| \\ &\leq \|\widehat{Q}_{k-1} \alpha_{k-1}^\square\| + \|\Delta I_{k-1} \alpha_{k-1}^\square\| \\ &\leq \begin{cases} \|\widehat{Q}_{k-1} \alpha_{k-1}^\square\| + \sqrt{s} \tilde{\gamma}_{n+s-2} \|\alpha_{k-1}^\square\| & \text{for Givens,} \\ \|\widehat{Q}_{k-1} \alpha_{k-1}^\square\| + \sqrt{s} \tilde{\gamma}_{ns} \|\alpha_{k-1}^\square\| & \text{for Householder.} \end{cases}\end{aligned}$$

Thus, we obtain the bounds

$$\begin{aligned}\|\alpha_{k-1}^\square\| &\leq \begin{cases} \|X_{k-1}\| + (1 + \gamma_1) \|X_k\| + \sqrt{s} ((1 + \tilde{\gamma}_{n+s-2}) \gamma_s + \tilde{\gamma}_{n+s-2}) \|\alpha_{k-1}^\square\|, \\ \|X_{k-1}\| + (1 + \gamma_1) \|X_k\| + \sqrt{s} ((1 + \tilde{\gamma}_{ns}) \gamma_s + \tilde{\gamma}_{ns}) \|\alpha_{k-1}^\square\| \end{cases} \\ &< \begin{cases} \|X_{k-1}\| + (1 + \gamma_1) \|X_k\| + \sqrt{s} \tilde{\gamma}_{n+2(s-1)} \|\alpha_{k-1}^\square\| & \text{for Givens,} \\ \|X_{k-1}\| + (1 + \gamma_1) \|X_k\| + \sqrt{s} \tilde{\gamma}_{(n+1)s} \|\alpha_{k-1}^\square\| & \text{for Householder.} \end{cases}\end{aligned}$$

Here, the second inequality is from

$$\begin{aligned}(1 + \tilde{\gamma}_{n+s-2}) \gamma_s + \tilde{\gamma}_{n+s-2} &< \tilde{\gamma}_s + \tilde{\gamma}_{n+s-2} + \tilde{\gamma}_s \tilde{\gamma}_{n+s-2} \quad (\because (22)) \\ &< \tilde{\gamma}_{n+2(s-1)} \quad (\because (21))\end{aligned}$$

and

$$\begin{aligned}(1 + \tilde{\gamma}_{ns}) \gamma_s + \tilde{\gamma}_{ns} &< \tilde{\gamma}_s + \tilde{\gamma}_{ns} + \tilde{\gamma}_s \tilde{\gamma}_{ns} \quad (\because (22)) \\ &< \tilde{\gamma}_{(n+1)s} \quad (\because (21))\end{aligned}$$

hold for Givens and Householder, respectively. Rearranging for α_{k-1}^\square , we have

$$\|\alpha_{k-1}^\square\| < \begin{cases} \frac{1}{1 - \sqrt{s} \tilde{\gamma}_{n+2(s-1)}} [\|X_{k-1}\| + (1 + \gamma_1) \|X_k\|] & \text{for Givens,} \\ \frac{1}{1 - \sqrt{s} \tilde{\gamma}_{(n+1)s}} [\|X_{k-1}\| + (1 + \gamma_1) \|X_k\|] & \text{for Householder.} \end{cases}$$

Here, $1 - \sqrt{s} \tilde{\gamma}_{n+2(s-1)} > 0$ and $1 - \sqrt{s} \tilde{\gamma}_{(n+1)s} > 0$ are equivalent to

$$c(n + 2(s - 1))(\sqrt{s} + 1)\mathbf{u} < 1 \quad \text{and} \quad c(n + 1)s(\sqrt{s} + 1)\mathbf{u} < 1,$$

respectively, and these are satisfied by the assumptions (26). Because the coefficients satisfy

$$\frac{1}{1 - \sqrt{s} \tilde{\gamma}_{n+2(s-1)}} = 1 + \frac{c(n + 2(s - 1))\sqrt{s}\mathbf{u}}{1 - c(n + 2(s - 1))(\sqrt{s} + 1)\mathbf{u}} < 1 + \tilde{\gamma}_{(n+2(s-1))(\sqrt{s}+1)}$$

and

$$\frac{1}{1 - \sqrt{s} \tilde{\gamma}_{(n+1)s}} = 1 + \frac{c(n + 1)s^{3/2}\mathbf{u}}{1 - c(n + 1)(\sqrt{s} + 1)s\mathbf{u}} < 1 + \tilde{\gamma}_{(n+1)(\sqrt{s}+1)s},$$

we obtain the bounds

$$\|\alpha_{k-1}^\square\| < \begin{cases} (1 + \tilde{\gamma}_{(n+2(s-1))(\sqrt{s}+1)}) [\|X_{k-1}\| + (1 + \gamma_1) \|X_k\|] & \text{for Givens,} \\ (1 + \tilde{\gamma}_{(n+1)(\sqrt{s}+1)s}) [\|X_{k-1}\| + (1 + \gamma_1) \|X_k\|] & \text{for Householder.} \end{cases}$$

Noting that

$$\begin{aligned}(1 + \tilde{\gamma}_{(n+2(s-1))(\sqrt{s}+1)})(1 + \gamma_1) &< 1 + \tilde{\gamma}_1 + \tilde{\gamma}_{(n+2(s-1))(\sqrt{s}+1)} + \tilde{\gamma}_1 \tilde{\gamma}_{(n+2(s-1))(\sqrt{s}+1)} \quad (\because (22)) \\ &< 1 + \tilde{\gamma}_{(n+2(s-1))(\sqrt{s}+1)+1} \quad (\because (21))\end{aligned}$$

and

$$\begin{aligned} (1 + \tilde{\gamma}_{(n+1)(\sqrt{s+1})s})(1 + \gamma_1) &< 1 + \tilde{\gamma}_1 + \tilde{\gamma}_{(n+1)(\sqrt{s+1})s} + \tilde{\gamma}_1 \tilde{\gamma}_{(n+1)(\sqrt{s+1})s} \quad (\because (22)) \\ &< 1 + \tilde{\gamma}_{(n+1)(\sqrt{s+1})s+1}, \quad (\because (21)) \end{aligned}$$

we obtain the final evaluations for α_{k-1}^\square as follows:

$$\|\alpha_{k-1}^\square\| < \begin{cases} (1 + \tilde{\gamma}_{(n+2(s-1))(\sqrt{s+1})})\|X_{k-1}\| \\ \quad + (1 + \tilde{\gamma}_{(n+2(s-1))(\sqrt{s+1})+1})\|X_k\| & \text{for Givens,} \\ (1 + \tilde{\gamma}_{(n+1)(\sqrt{s+1})s})\|X_{k-1}\| \\ \quad + (1 + \tilde{\gamma}_{(n+1)(\sqrt{s+1})s+1})\|X_k\| & \text{for Householder.} \end{cases} \quad (31)$$

Now, to evaluate $\|E_{X_k}^\square\|$ simply, we use the bounds

$$\begin{aligned} \gamma_s(1 + \tilde{\gamma}_{(n+2(s-1))(\sqrt{s+1})+1}) &= \gamma_s + \gamma_s \tilde{\gamma}_{(n+2(s-1))(\sqrt{s+1})+1} < \gamma_s + \gamma_s = 2\gamma_s, \\ \gamma_s(1 + \tilde{\gamma}_{(n+1)(\sqrt{s+1})s+1}) &= \gamma_s + \gamma_s \tilde{\gamma}_{(n+1)(\sqrt{s+1})s+1} < \gamma_s + \gamma_s = 2\gamma_s, \end{aligned}$$

where the inequalities are from (23), and the corresponding assumptions (26) are imposed for Givens and Householder, respectively. Following a similar argument to the above bounds, substituting (31) into the bounds (30) of $\|E_{X_k}^\square\|$ gives

$$\begin{aligned} \|E_{X_k}^\square\| &< \begin{cases} 2\sqrt{s}(1 + \tilde{\gamma}_{n+s-2})\gamma_s(\|X_{k-1}\| + \|X_k\|) & \text{for Givens,} \\ 2\sqrt{s}(1 + \tilde{\gamma}_{ns})\gamma_s(\|X_{k-1}\| + \|X_k\|) & \text{for Householder} \end{cases} \quad (32) \\ &< 4\sqrt{s}\gamma_s(\|X_{k-1}\| + \|X_k\|). \end{aligned}$$

Summing up (29) and (32), we obtain the bound (27).

Next, it holds that $\|E'_{R_k}\| \leq \gamma_1 \|R_k\|$ as in (29). From (18), (19), (23), and (31), similarly to (32), we obtain the following bound:

$$\begin{aligned} \|E'_{R_k}\| &\leq \gamma_s \|\text{fl}(A\hat{Q}_{k-1})\| \|\alpha_{k-1}^\square\| \\ &< \begin{cases} \gamma_s(\|A\hat{Q}_{k-1}\| + \gamma_m \|A\| \|\hat{Q}_{k-1}\|) [(1 + \tilde{\gamma}_{(n+2(s-1))(\sqrt{s+1})})\|X_{k-1}\| \\ \quad + (1 + \tilde{\gamma}_{(n+2(s-1))(\sqrt{s+1})+1})\|X_k\|] & \text{for Givens,} \\ \gamma_s(\|A\hat{Q}_{k-1}\| + \gamma_m \|A\| \|\hat{Q}_{k-1}\|) [(1 + \tilde{\gamma}_{(n+1)(\sqrt{s+1})s})\|X_{k-1}\| \\ \quad + (1 + \tilde{\gamma}_{(n+1)(\sqrt{s+1})s+1})\|X_k\|] & \text{for Householder} \end{cases} \\ &< 2\gamma_s(1 + \gamma_m) \|A\| \|\hat{Q}_{k-1}\| (\|X_{k-1}\| + \|X_k\|) \\ &< \begin{cases} 4\sqrt{s}\gamma_s(1 + \tilde{\gamma}_{n+s-2}) \|A\| (\|X_{k-1}\| + \|X_k\|) & \text{for Givens,} \\ 4\sqrt{s}\gamma_s(1 + \tilde{\gamma}_{ns}) \|A\| (\|X_{k-1}\| + \|X_k\|) & \text{for Householder} \end{cases} \\ &< 8\sqrt{s}\gamma_s \|A\| (\|X_{k-1}\| + \|X_k\|). \end{aligned}$$

From (19), in a similar fashion to the bounds above, we have

$$\begin{aligned} \|E''_{R_k} \alpha_{k-1}^\square\| &\leq \gamma_m \|A\| \|\hat{Q}_{k-1}\| \|\alpha_{k-1}^\square\| \\ &< 2\gamma_m \|A\| \|\hat{Q}_{k-1}\| (\|X_{k-1}\| + \|X_k\|) \\ &< 4\sqrt{s}\gamma_m \|A\| (\|X_{k-1}\| + \|X_k\|). \end{aligned}$$

Hence, summing up the bounds for $\|E'_{R_k}\|$, $\|E_{R_k}^\square\|$, and $\|E''_{R_k} \alpha_{k-1}^\square\|$ gives (28). \square

4.3 Bound for the residual gap

We provide a proof of Theorem 4.1 under the assumptions in Lemma 4.1.

Proof of Theorem 4.1. From Lemma 4.1, we have that

$$\begin{aligned}
\|G_{R_k}\| &= \|[B - A(X_{k-1} + \widehat{Q}_{k-1}\alpha_{k-1}^\square + E_{X_k})] - (R_{k-1} - A\widehat{Q}_{k-1}\alpha_{k-1}^\square - E_{R_k})\| \\
&\leq \|(B - AX_{k-1}) - R_{k-1}\| + \|A\| \|E_{X_k}\| + \|E_{R_k}\| \\
&\leq \|A\| \sum_{i=1}^k \|E_{X_i}\| + \sum_{i=1}^k \|E_{R_i}\| \\
&< 4\sqrt{s}\gamma_s \|A\| \sum_{i=1}^k (\|X_{i-1}\| + \|X_i\|) + \gamma_1 \|A\| \sum_{i=1}^k \|X_i\| \\
&\quad + \gamma_1 \sum_{i=1}^k \|R_i\| + 4\sqrt{s}(\gamma_m + 2\gamma_s) \|A\| \sum_{i=1}^k (\|X_{i-1}\| + \|X_i\|) \\
&< [8\sqrt{s}(\gamma_m + 3\gamma_s) + \gamma_1] \|A\| \sum_{i=1}^k \|X_i\| + \gamma_1 \sum_{i=1}^k \|R_i\| \\
&< (8\sqrt{s}\gamma_{m+3s} + \gamma_1)k \|A\| \max_{0 < i \leq k} \|X_i\| + k\gamma_1 \max_{0 < i \leq k} \|R_i\|.
\end{aligned}$$

□

5 Concluding remarks

In this study, we have proposed a block version of the cross-interactive residual smoothing (Algorithm 2 referred to as BI-CIRS) incorporated with Lanczos-type solvers for linear systems with multiple right-hand sides. The proposed smoothing scheme can obtain a monotonically decreasing sequence of the residual norms along with a smoothly increasing sequence of the associated approximation norms, thereby reducing the residual gap and improving the attainable accuracy of the approximations. The key point of the block version is to define the smoothing parameter as an s -by- s matrix and orthonormalize the columns of n -by- s auxiliary matrices used to update the approximations and residuals. We have demonstrated the performance of the proposed scheme through numerical experiments in section 3. The rounding error analysis in Theorem 4.1 shows that BI-CIRS is useful in avoiding a large residual gap, even when allowing inexactness of the orthonormalization, which is weaker than our previous assumption made in [1, Theorem 2.2].

This study presented culminating results on CIRS for reducing the residual gap. Nevertheless, we will continue the quest for further advances from both theoretical and experimental viewpoints in future studies. In the future, we could consider preconditioned and/or complex arithmetic cases and reduce the computational costs by a partial application of the orthonormalization for BI-CIRS (cf. [1, section 7.5]).

A Towards general case of orthonormalizations

Beyond using a particular process for the orthonormalization strategy as discussed in section 4, we consider the residual gap in a more general case. The quantity $\|\Delta I_{k-1}\|$ below is regarded as the relative distance from a column-orthonormal matrix Q_{k-1} closest to \widehat{Q}_{k-1} .

Lemma A.1. *Let $X_k \in \mathbb{F}^{n \times s}$ and $R_k \in \mathbb{F}^{n \times s}$ be the k th approximation and residual, respectively, generated by (15) in finite precision arithmetic. Let $\widehat{Q}_{k-1} \in \mathbb{R}^{n \times s}$ be a numerically computed Q -factor of the QR decomposition of P_{k-1} such that $\widehat{Q}_{k-1} = Q_{k-1}(I_s + \Delta I_{k-1})$ for some $Q_{k-1} \in \mathbb{R}^{n \times s}$ whose columns are exactly orthonormal. Assume that m , s , and \mathbf{u} satisfy*

$$\|\Delta I_{k-1}\| + \gamma_s \|\widehat{Q}_{k-1}\| < 1 \quad \text{and} \quad (m + s)\mathbf{u} < 1. \quad (33)$$

Then, the local errors are bounded as

$$\|E_{X_k}\| \leq \frac{\gamma_s \|\widehat{Q}_{k-1}\|}{1 - \gamma_s \|\widehat{Q}_{k-1}\| - \|\Delta I_{k-1}\|} [\|X_{k-1}\| + (1 + \gamma_1)\|X_k\|] + \gamma_1 \|X_k\|, \quad (34)$$

$$\|E_{R_k}\| \leq \gamma_1 \|R_k\| + \frac{\gamma_{m+s} \|A\| \|\widehat{Q}_{k-1}\|}{1 - \gamma_s \|\widehat{Q}_{k-1}\| - \|\Delta I_{k-1}\|} [\|X_{k-1}\| + (1 + \gamma_1)\|X_k\|]. \quad (35)$$

Proof. As in (29), we have

$$\|E'_{X_k}\| \leq \gamma_1 \|X_k\|, \quad (36)$$

and it follows from (18) that $\|E_{X_k}^\square\| \leq \gamma_s \|\widehat{Q}_{k-1}\| \|\alpha_{k-1}^\square\|$. Then, from (25), we have

$$\begin{aligned} \|\widehat{Q}_{k-1} \alpha_{k-1}^\square\| &\leq \|X_{k-1}\| + \|X_k\| + \|E'_{X_k}\| + \|E_{X_k}^\square\| \\ &\leq \|X_{k-1}\| + (1 + \gamma_1)\|X_k\| + \gamma_s \|\widehat{Q}_{k-1}\| \|\alpha_{k-1}^\square\|. \end{aligned}$$

Plugging this into

$$\begin{aligned} \|\alpha_{k-1}^\square\| &= \|Q_{k-1} \alpha_{k-1}^\square\| = \|(\widehat{Q}_{k-1} - Q_{k-1} \Delta I_{k-1}) \alpha_{k-1}^\square\| \\ &\leq \|\widehat{Q}_{k-1} \alpha_{k-1}^\square\| + \|\Delta I_{k-1}\| \|\alpha_{k-1}^\square\|, \end{aligned}$$

it holds that

$$\|\alpha_{k-1}^\square\| \leq \|X_{k-1}\| + (1 + \gamma_1)\|X_k\| + (\gamma_s \|\widehat{Q}_{k-1}\| + \|\Delta I_{k-1}\|) \|\alpha_{k-1}^\square\|.$$

We therefore obtain the bound for α_{k-1}^\square as

$$\|\alpha_{k-1}^\square\| \leq \frac{1}{1 - \gamma_s \|\widehat{Q}_{k-1}\| - \|\Delta I_{k-1}\|} [\|X_{k-1}\| + (1 + \gamma_1)\|X_k\|], \quad (37)$$

where the denominator is positive from the first assumption in (33). Hence, we have

$$\|E_{X_k}^\square\| \leq \frac{\gamma_s \|\widehat{Q}_{k-1}\|}{1 - \gamma_s \|\widehat{Q}_{k-1}\| - \|\Delta I_{k-1}\|} [\|X_{k-1}\| + (1 + \gamma_1)\|X_k\|]. \quad (38)$$

Summing up (36) and (38), we obtain the bound (34).

Next, from $\|E'_{R_k}\| \leq \gamma_1 \|R_k\|$, (18), (19), and (37), we have

$$\begin{aligned} \|E_{R_k}^\square\| &\leq \gamma_s \|\mathfrak{f}(A \widehat{Q}_{k-1})\| \|\alpha_{k-1}^\square\| \\ &\leq \frac{\gamma_s}{1 - \gamma_s \|\widehat{Q}_{k-1}\| - \|\Delta I_{k-1}\|} (\|A \widehat{Q}_{k-1}\| + \gamma_m \|A\| \|\widehat{Q}_{k-1}\|) [\|X_{k-1}\| + (1 + \gamma_1)\|X_k\|] \\ &\leq \frac{\gamma_s (1 + \gamma_m) \|A\| \|\widehat{Q}_{k-1}\|}{1 - \gamma_s \|\widehat{Q}_{k-1}\| - \|\Delta I_{k-1}\|} [\|X_{k-1}\| + (1 + \gamma_1)\|X_k\|]. \end{aligned}$$

From (19), $\|E_{R_k}''' \alpha_{k-1}^\square\| \leq \gamma_m \|A\| \|\widehat{Q}_{k-1}\| \|\alpha_{k-1}^\square\|$ also holds. Hence, we have

$$\begin{aligned} \|E_{R_k}\| &\leq \gamma_1 \|R_k\| + \frac{\gamma_s (1 + \gamma_m) \|A\| \|\widehat{Q}_{k-1}\|}{1 - \gamma_s \|\widehat{Q}_{k-1}\| - \|\Delta I_{k-1}\|} [\|X_{k-1}\| + (1 + \gamma_1)\|X_k\|] \\ &\quad + \frac{\gamma_m \|A\| \|\widehat{Q}_{k-1}\|}{1 - \gamma_s \|\widehat{Q}_{k-1}\| - \|\Delta I_{k-1}\|} [\|X_{k-1}\| + (1 + \gamma_1)\|X_k\|] \\ &\leq \gamma_1 \|R_k\| + \frac{\gamma_{m+s} \|A\| \|\widehat{Q}_{k-1}\|}{1 - \gamma_s \|\widehat{Q}_{k-1}\| - \|\Delta I_{k-1}\|} [\|X_{k-1}\| + (1 + \gamma_1)\|X_k\|]. \end{aligned}$$

Here, the inequality $\gamma_s (1 + \gamma_m) + \gamma_m \leq \gamma_{m+s}$ and the second assumption in (33) are used. \square

Finally, we evaluate the residual gap by using Lemma A.1. The following result generalizes those for Givens and Householder orthonormalizations in section 4 by retaining $\|\widehat{Q}_{k-1}\|$, and thus other orthonormalization results such as from the Gram–Schmidt process are expected to be incorporated.

Theorem A.1. *Under the assumptions in Lemma A.1 with $X_0 = O$ and*

$$\|\Delta I_i\| + \gamma_s \|\widehat{Q}_i\| < 1 \quad \text{for } i < k, \quad \text{and } (m+2s)\mathbf{u} < 1,$$

the norm of the residual gap $G_{R_k} := (B - AX_k) - R_k$ is bounded as follows:

$$\|G_{R_k}\| < \sum_{i=1}^k \frac{2\gamma_{m+2s}\|A\|\|\widehat{Q}_{i-1}\|}{1 - \gamma_s\|\widehat{Q}_{i-1}\| - \|\Delta I_{i-1}\|} (\|X_{i-1}\| + \|X_i\|) + \gamma_1\|A\| \sum_{i=1}^k \|X_i\| + \gamma_1 \sum_{i=1}^k \|R_i\|. \quad (39)$$

Proof. From Lemma A.1, we have that

$$\begin{aligned} \|G_{R_k}\| &\leq \|A\| \sum_{i=1}^k \|E_{X_i}\| + \sum_{i=1}^k \|E_{R_k}\| \\ &\leq \sum_{i=1}^k \frac{\gamma_s\|A\|\|\widehat{Q}_{i-1}\|}{1 - \gamma_s\|\widehat{Q}_{i-1}\| - \|\Delta I_{i-1}\|} [\|X_{i-1}\| + (1 + \gamma_1)\|X_i\|] + \gamma_1\|A\| \sum_{i=1}^k \|X_i\| \\ &\quad + \gamma_1 \sum_{i=1}^k \|R_i\| + \sum_{i=1}^k \frac{\gamma_{m+s}\|A\|\|\widehat{Q}_{i-1}\|}{1 - \gamma_s\|\widehat{Q}_{i-1}\| - \|\Delta I_{i-1}\|} [\|X_{i-1}\| + (1 + \gamma_1)\|X_i\|] \\ &< \sum_{i=1}^k \frac{2\gamma_{m+2s}\|A\|\|\widehat{Q}_{i-1}\|}{1 - \gamma_s\|\widehat{Q}_{i-1}\| - \|\Delta I_{i-1}\|} (\|X_{i-1}\| + \|X_i\|) + \gamma_1\|A\| \sum_{i=1}^k \|X_i\| + \gamma_1 \sum_{i=1}^k \|R_i\|, \end{aligned}$$

where $(\gamma_s + \gamma_{m+s})(1 + \gamma_1) < 2(\gamma_s + \gamma_{m+s}) < 2\gamma_{m+2s}$ is used. \square

It is an important observation in (39) that the distance $\|\Delta I_{i-1}\|$ is in the denominator, and thus the upper bound of the residual gap can be large if $\|\Delta I_{i-1}\|$ becomes large. This also implies that, when using the recursion formulas (5) without the orthonormalization (as an extreme case), the residual gap may increase even if smooth convergence behaviors of the residual and approximation norms are obtained; such a phenomenon is often observed in numerical experiments (e.g., see Figure 1c).

References

- [1] K. AIHARA, A. IMAKURA, AND K. MORIKUNI, *Cross-interactive residual smoothing for global and block Lanczos-type solvers for linear systems with multiple right-hand sides*, SIAM J. Matrix Anal. Appl., 43 (2022), pp. 1308–1330, <https://doi.org/10.1137/21M1436774>.
- [2] K. AIHARA, R. KOMEYAMA, AND E. ISHIWATA, *Variants of residual smoothing with a small residual gap*, BIT, 59 (2019), pp. 565–584, <https://doi.org/10.1007/s10543-019-00751-w>.
- [3] T. F. CHAN AND M. K. NG, *Galerkin projection methods for solving multiple linear systems*, SIAM J. Sci. Comput., 21 (1999), pp. 836–850, <https://doi.org/10.1137/s1064827598310227>.
- [4] T. F. CHAN AND W. L. WAN, *Analysis of projection methods for solving linear systems with multiple right-hand sides*, SIAM J. Sci. Comput., 18 (1997), pp. 1698–1721, <https://doi.org/10.1137/s1064827594273067>.

- [5] D. C. CHATFIELD, M. S. REEVES, D. G. TRUHLAR, C. DUNECZKY, AND D. W. SCHWENKE, *Complex generalized minimal residual algorithm for iterative solution of quantum-mechanical reactive scattering equations*, J. Chem. Phys., 97 (1992), pp. 8322–8333, <https://doi.org/10.1063/1.463402>.
- [6] J. CULLUM, *The simultaneous computation of a few of the algebraically largest and smallest eigenvalues of a large, sparse, symmetric matrix*, BIT, 18 (1978), pp. 265–275, <https://doi.org/10.1007/bf01930896>.
- [7] T. A. DAVIS AND Y. HU, *The University of Florida sparse matrix collection*, ACM Trans. Math. Softw., 38 (2011), pp. 1–25, <https://doi.org/10.1145/2049662.2049663>.
- [8] L. DU, T. SOGABE, B. YU, Y. YAMAMOTO, AND S.-L. ZHANG, *A block IDR(s) method for nonsymmetric linear systems with multiple right-hand sides*, Journal of Computational and Applied Mathematics, 235 (2011), pp. 4095–4106, <https://doi.org/10.1016/j.cam.2011.02.035>.
- [9] A. A. DUBRULLE, *Retooling the method of block conjugate gradients*, Electron. Trans. Numer. Anal., 12 (2001), pp. 216–233.
- [10] A. EL GUENNOUNI, K. JBILOU, AND H. SADOK, *A block version of BiCGSTAB for linear systems with multiple right-hand sides*, Electron. Trans. Numer. Anal., 16 (2003), pp. 129–142.
- [11] A. EL GUENNOUNI, K. JBILOU, AND H. SADOK, *The block Lanczos method for linear systems with multiple right-hand sides*, Appl. Numer. Math., 51 (2004), pp. 243–256, <https://doi.org/10.1016/j.apnum.2004.04.001>.
- [12] R. W. FREUND AND M. MALHOTRA, *A block QMR algorithm for non-Hermitian linear systems with multiple right-hand sides*, Linear Algebra Appl., 254 (1997), pp. 119–157, [https://doi.org/10.1016/s0024-3795\(96\)00529-0](https://doi.org/10.1016/s0024-3795(96)00529-0).
- [13] G. H. GOLUB, D. RUIZ, AND A. TOUHAMI, *A hybrid approach combining Chebyshev filter and conjugate gradient for solving linear systems with multiple right-hand sides*, SIAM J. Matrix Anal. Appl., 29 (2007), pp. 774–795, <https://doi.org/10.1137/060649458>.
- [14] G. H. GOLUB AND R. R. UNDERWOOD, *The block Lanczos method for computing eigenvalues*, in Mathematical Software, Elsevier, 1977, pp. 361–377, <https://doi.org/10.1016/b978-0-12-587260-7.50018-2>.
- [15] A. GREENBAUM, *Estimating the attainable accuracy of recursively computed residual methods*, SIAM J. Matrix Anal. Appl., 18 (1997), pp. 535–551, <https://doi.org/10.1137/S0895479895284944>.
- [16] M. H. GUTKNECHT AND M. ROZLOŽNÍK, *Residual smoothing techniques: Do they improve the limiting accuracy of iterative solvers?*, BIT, 41 (2001), pp. 86–114, <https://doi.org/10.1023/a:1021917801600>.
- [17] N. J. HIGHAM, *Accuracy and Stability of Numerical Algorithms*, SIAM, Philadelphia, PA, 2nd ed., 2002.
- [18] T. IKEGAMI AND T. SAKURAI, *Contour integral eigensolver for non-Hermitian systems: A Rayleigh–Ritz-type approach*, Taiwanese J. Math., 14 (2010), pp. 825–837, <https://doi.org/10.11650/twjmath/1500405869>.
- [19] T. IKEGAMI, T. SAKURAI, AND U. NAGASHIMA, *A filter diagonalization for generalized eigenvalue problems based on the Sakurai–Sugiura projection method*, J. Comput. Appl. Math., 233 (2010), pp. 1927–1936, <https://doi.org/10.1016/j.cam.2009.09.029>.

- [20] K. JBILOU, *Smoothing iterative block methods for linear systems with multiple right-hand sides*, J. Comput. Appl. Math., 107 (1999), pp. 97–109, [https://doi.org/10.1016/s0377-0427\(99\)00083-7](https://doi.org/10.1016/s0377-0427(99)00083-7).
- [21] K. JBILOU, A. MESSAOUDI, AND H. SADOK, *Global FOM and GMRES algorithms for matrix equations*, Appl. Numer. Math., 31 (1999), pp. 49–63, [https://doi.org/10.1016/S0168-9274\(98\)00094-4](https://doi.org/10.1016/S0168-9274(98)00094-4).
- [22] K. JBILOU, H. SADOK, AND A. TINZEFTE, *Oblique projection methods for linear systems with multiple right-hand sides*, Electron. Trans. Numer. Anal., 20 (2005), pp. 119–138.
- [23] R. KOMEYAMA, K. AIHARA, AND E. ISHIWATA, *Reconsideration of residual smoothing technique for improving the accuracy of approximate solutions of CGS-type iterative methods*, Trans. Japan Soc. Ind. Appl. Math., 28 (2018), pp. 18–38, https://doi.org/10.11540/jsiamt.28.1_18.
- [24] R. KURAMOTO AND H. TADANO, *Accuracy improvement of the block product-type iterative methods for linear systems with multiple right-hand sides*, Trans. Japan Soc. Ind. Appl. Math., 30 (2020), pp. 290–319, https://doi.org/10.11540/jsiamt.30.4_290.
- [25] M. MALHOTRA, R. W. FREUND, AND P. M. PINSKY, *Iterative solution of multiple radiation and scattering problems in structural acoustics using a block quasi-minimal residual algorithm*, Comput. Methods Appl. Mech. Engrg., 146 (1997), pp. 173–196, [https://doi.org/10.1016/s0045-7825\(96\)01227-3](https://doi.org/10.1016/s0045-7825(96)01227-3).
- [26] E. K. MILLER, *Assessing the impact of large-scale computing on the size and complexity of first-principles electromagnetic models*, in Directions in Electromagnetic Wave Modeling, Springer US, 1991, pp. 185–196, https://doi.org/10.1007/978-1-4899-3677-6_19.
- [27] M. NAITO, H. TADANO, AND T. SAKURAI, *A modified block IDR(s) method for computing high accuracy solutions*, JSIAM Lett., 4 (2012), pp. 25–28, <https://doi.org/10.14495/jsiaml.4.25>.
- [28] Y. NAKAMURA, K.-I. ISHIKAWA, Y. KURAMASHI, T. SAKURAI, AND H. TADANO, *Modified block BiCGSTAB for lattice QCD*, Comput. Phys. Commun., 183 (2012), pp. 34–37, <https://doi.org/10.1016/j.cpc.2011.08.010>.
- [29] A. A. NIKISHIN AND A. Y. YEREMIN, *Variable block CG algorithms for solving large sparse symmetric positive definite linear systems on parallel computers, I: General iterative scheme*, SIAM J. Matrix Anal. Appl., 16 (1995), pp. 1135–1153, <https://doi.org/10.1137/s0895479893247679>.
- [30] D. P. O’LEARY, *The block conjugate gradient algorithm and related methods*, Linear Algebra Appl., 29 (1980), pp. 293–322, [https://doi.org/10.1016/0024-3795\(80\)90247-5](https://doi.org/10.1016/0024-3795(80)90247-5).
- [31] M. PAPADRAKAKIS AND S. SMEROU, *A new implementation of the Lanczos method in linear problems*, Internat. J. Numer. Methods Engrg., 29 (1990), pp. 141–159, <https://doi.org/10.1002/nme.1620290110>.
- [32] E. POLIZZI, *Density-matrix-based algorithm for solving eigenvalue problems*, Phys. Rev. B, 79 (2009), 115112, <https://doi.org/10.1103/physrevb.79.115112>.
- [33] S. RASHEDI, G. EBADI, S. BIRK, AND A. FROMMER, *On short recurrence Krylov type methods for linear systems with many right-hand sides*, J. Comput. Appl. Math., 300 (2016), pp. 18–29, <https://doi.org/10.1016/j.cam.2015.11.040>.
- [34] Y. SAAD, *On the Lanczos method for solving symmetric linear systems with several right-hand sides*, Math. Comp., 48 (1987), pp. 651–651, <https://doi.org/10.1090/s0025-5718-1987-0878697-3>.

- [35] S. SAITO, H. TADANO, AND A. IMAKURA, *Development of the block BiCGSTAB(ℓ) method for solving linear systems with multiple right hand sides*, JSIAM Lett., 6 (2014), pp. 65–68, <https://doi.org/10.14495/jsiaml.6.65>.
- [36] T. SAKURAI, H. TADANO, AND Y. KURAMASHI, *Application of block Krylov subspace algorithms to the Wilson–Dirac equation with multiple right-hand sides in lattice QCD*, Comput. Phys. Commun., 181 (2010), pp. 113–117, <https://doi.org/10.1016/j.cpc.2009.09.006>.
- [37] W. SCHÖNAUER, *Scientific Computing on Vector Computers*, Elsevier, Amsterdam, 1987.
- [38] V. SIMONCINI, *A stabilized QMR version of block BiCG*, SIAM J. Matrix Anal. Appl., 18 (1997), pp. 419–434, <https://doi.org/10.1137/s0895479894264673>.
- [39] G. L. G. SLEIJPEN, A. G. L. BOOTEN, D. R. FOKKEMA, AND H. A. VAN DER VORST, *Jacobi–Davidson type methods for generalized eigenproblems and polynomial eigenproblems*, BIT, 36 (1996), pp. 595–633, <https://doi.org/10.1007/bf01731936>.
- [40] C. F. SMITH, *The performance of preconditioned iterative methods in computational electromagnetics*, PhD thesis, Dept. of Electrical Engineering, Univ. of Illinois at Urbana-Champaign, 1987.
- [41] C. F. SMITH, A. F. PETERSON, AND R. MITTRA, *A conjugate gradient algorithm for the treatment of multiple incident electromagnetic fields*, IEEE Trans. Antennas and Propagation, 37 (1989), pp. 1490–1493, <https://doi.org/10.1109/8.43571>.
- [42] C. F. SMITH, A. F. PETERSON, AND R. MITTRA, *The biconjugate gradient method for electromagnetic scattering*, IEEE Trans. Antennas and Propagation, 38 (1990), pp. 938–940, <https://doi.org/10.1109/8.55595>.
- [43] H. TADANO, *Development of the block BiCGGR2 method for linear systems with multiple right-hand sides*, Jpn. J. Ind. Appl. Math., 36 (2019), pp. 563–577, <https://doi.org/10.1007/s13160-019-00354-6>.
- [44] H. TADANO, Y. KURAMASHI, AND T. SAKURAI, *Application of preconditioned block BiCGGR to the Wilson–Dirac equation with multiple right-hand sides in lattice QCD*, Comput. Phys. Commun., 181 (2010), pp. 883–886, <https://doi.org/10.1016/j.cpc.2009.12.025>.
- [45] H. TADANO, T. SAKURAI, AND Y. KURAMASHI, *Block BiCGGR: a new block Krylov subspace method for computing high accuracy solutions*, JSIAM Lett., 1 (2009), pp. 44–47, <https://doi.org/10.14495/jsiaml.1.44>.
- [46] A. TAHERIAN AND F. TOUTOUNIAN, *Block GPBi-CG method for solving nonsymmetric linear systems with multiple right-hand sides and its convergence analysis*, Numer. Algorithms, 88 (2021), pp. 1831–1850, <https://doi.org/10.1007/s11075-021-01097-7>.
- [47] H. F. WALKER, *Residual smoothing and peak/plateau behavior in Krylov subspace methods*, Appl. Numer. Math., 19 (1995), pp. 279–286, [https://doi.org/10.1016/0168-9274\(95\)00087-9](https://doi.org/10.1016/0168-9274(95)00087-9).
- [48] R. WEISS, *Properties of generalized conjugate gradient methods*, Numer. Linear Algebra Appl., 1 (1994), pp. 45–63, <https://doi.org/10.1002/nla.1680010106>.
- [49] R. WEISS, *Parameter-free iterative linear solvers*, Akademie Verlag, Berlin, 1996.
- [50] W. YANG AND W. H. MILLER, *Block Lanczos approach combined with matrix continued fraction for the S-matrix Kohn variational principle in quantum scattering*, J. Chem. Phys., 91 (1989), pp. 3504–3508, <https://doi.org/10.1063/1.456880>.
- [51] J. ZHANG AND F. DAI, *Global CGS algorithm for linear systems with multiple right-hand sides*, Numer. Math. J. Chinese Univ., 30 (2008), pp. 390–399.

- [52] J. ZHANG, H. DAI, AND J. ZHAO, *Generalized global conjugate gradient squared algorithm*, Appl. Math. Comput., 216 (2010), pp. 3694–3706, <https://doi.org/10.1016/j.amc.2010.05.026>.
- [53] L. ZHOU AND H. F. WALKER, *Residual smoothing techniques for iterative methods*, SIAM J. Sci. Comput., 15 (1994), pp. 297–312, <https://doi.org/10.1137/0915021>.